Journal of Materials Chemistry B

Accepted Manuscript

This is an *Accepted Manuscript*, which has been through the Royal Society of Chemistry peer review process and has been accepted for publication.

Accepted Manuscripts are published online shortly after acceptance, before technical editing, formatting and proof reading. Using this free service, authors can make their results available to the community, in citable form, before we publish the edited article. We will replace this *Accepted Manuscript* with the edited and formatted *Advance Article* as soon as it is available.

You can find more information about *Accepted Manuscripts* in the Information for Authors.

Please note that technical editing may introduce minor changes to the text and/or graphics, which may alter content. The journal's standard Terms & Conditions and the Ethical guidelines still apply. In no event shall the Royal Society of Chemistry be held responsible for any errors or omissions in this *Accepted Manuscript* or any consequences arising from the use of any information it contains.

ROYAL SOCIETY OF CHEMISTRY

www.rsc.org/materialsB

Please do not adjust margins

Journal Name

ARTICLE

Narrow Band Gap Conjugated Polyelectrolytes for Photothermal Killing of Bacteria

Received 00th January 20xx,
Accepted 00th January 20xx

DOI: 10.1039/x0xx00000x

www.rsc.org/

Guangxue Feng,[a,b] Cheng-Kang Mai,[c] Ruoyu Zhan,[a] Guillermo C. Bazan,*[c] and Bin Liu*[a]

We report the demonstration of antimicrobial conjugated polyelectrolytes (CPEs) with high NIR absorbance for selective and efficient photothermal killing of bacteria over mammalian cells. The antimicrobial CPE possessing quaternary ammonium (QA) terminated side chains (**P1**) shows higher binding preference and more dark toxicity towards Gram-positive and Gram-negative bacteria over mammalian cells. Bestowed by π-conjugated backbones, **P1** exhibits a high molar absorptivity of 39.8 $Lg^{-1}cm^{-1}$ at 808 nm with an efficient photothermal conversion efficiency of 33±1%. Upon 808 nm laser irradiation, **P1** shows enhanced bactericidal effects, but not to mammalian cells. Although the anionic CPE counterpart with the same polymer backbone but sulfonate terminated side chains (**P2**) possesses similar photothermal conversion ability, it exhibits much lower antibacterial effects due to its low binding affinity. This study thus reveals that bacteria-CPE electrostatic interaction plays a major role in bacteria recognition although the hydrophobic interaction also contributes.

Introduction

There are increased concerns about pathogen bacterial infections that increase morbidity and mortality in clinical practice.[1] As a promising alternative of antibiotics, antimicrobial polyelectrolytes (AMPs) have been developed and utilized for the treatment of pathogen infections.[2] Their amphiphilic structures, molecular weights, and charged functional groups, such as quaternary ammonium (QA) salts, play critical roles in bacteria recognition, membrane disruption, and antimicrobial function.[3] However, as the main part of AMPs, the backbones mainly served as the manipulator to control the chain length, percentages of different repeating units, and charged group density, while the backbones themselves minimally contributed to the antimicrobial activity. Therefore, the developed AMPs are usually integrated with antimicrobial organic or inorganic compounds to further enhance their killing efficiency towards pathogen bacteria.[4] As a consequence, it is relevant to design, prepare and test novel AMPs with new backbones that could also provide antimicrobial functions.

Conjugated polyelectrolytes (CPEs) are a class of macromolecules that contain a π-conjugated backbone and pendant ionic side chains.[5] The delocalized electronic structure structures bestow these materials with semiconducting and light-harvesting properties. CPEs have therefore been integrated into a wide range of applications, including optoelectronic devices,[5c,6] biosensors,[7] and bioimaging protocols.[8] Due to lack of binding affinity towards bacteria, prior work of CPE on antimicrobial applications is limited.[9] CPE variations with QA containing side chains were recently reported to exhibit high antimicrobial activities against various bacteria.[10] These antimicrobial CPEs are able to generate reactive oxygen species (ROS) under irradiation and subsequently oxidize bacteria cell walls. However, the majority of CPEs exhibit absorption and emission within the visible region of the spectrum. Shifting the absorption profile to near-infrared (NIR) regions should enable additional function where penetration of light into deep tissue is desirable. One specific interest is in photothermal therapy (PTT), where non-radiative vibrational relaxation of the excitation is used to generate a local heating event.[11] The generated heat could lead to the ablation and destruction of cancer cells or bacteria. Up to now, various photothermal reagents, including gold nanoparticles or nanorods, graphene oxides and carbon nanotubes have been widely applied in PTT, however, the non-biodegradable nature of these inorganic material greatly hampered their practical applications.[12]

A recent class of water-soluble, narrow band gap CPEs contains many of the desirable attributes described above. Specifically, **P1** and **P2** (see Fig. 1A) have the same backbone structure, but contain oppositely charged end groups, e.g. **P1** has cationic QA substituents, while **P2** has anionic sulfonate groups. Having the identical backbone in both systems provides us with the ability to carry out comparative studies that yield insight into hydrophobic and/or electrostatic

[a] *Department of Chemical and Biomolecular Engineering, National University of Singapore, 4 Engineering Drive 4, Singapore 117585. E-mail: cheliub@nus.edu.sg.*
[b] *Environmental Research Institute, National University of Singapore, Singapore, 117411.*
[c] *Center for Polymers and Organic Solids, Department of Chemistry and Biochemistry, University of California, Santa Barbara, CA 93106, USA. E-mail: bazan@chem.ucsb.edu*
† Electronic Supplementary Information (ESI) available: See
DOI: 10.1039/x0xx00000x

Journal of Materials Chemistry B Accepted Manuscript

contributions to bacteria-CPE interactions. In addition, that **P1** is a polycation, in combination with its low emission efficiency and high molar absorptivity at longer wavelengths, provides us with the opportunity to begin understanding molecular-bacteria interactions that lead to efficient photothermal bactericidal effects. We thus describe in this contribution the first examination of photothermal effect in CPEs. We further demonstrate a higher binding affinity between the cationic **P1** and bacteria, relative to anionic **P2**, and selectivity preferences between Gram-positive and Gram-negative bacteria/mammalian cells. This set of studies provides a perspective of overall anti-bacterial action of relevance within the content of new strategies to fight bacterial infections. It is worth recalling that the prevalence of antibiotic resistance strains and emergence of drug resistance bacteria are impeding the treatment of bacterial infections,[13] new antibacterial therapeutic reagents are thus highly desirable for practical clinical applications.

Results and discussion

As shown in Fig. 1A, **P1** and **P2** share a backbone that comprises alternating 4,4-bis-alkyl-4H-cyclopenta-[2,1-b;3,4-b']-dithiophene and 2,1,3-benzothiadiazole structural units. **P1** shows two absorption peaks centered at 424 and 736 nm, while **P2** possesses two blue-shifted absorption peaks centered at 410 and 715 nm, respectively (Fig. 1B). It should be noted that **P2** also exhibits a broad, low-energy transition starting from 900 nm, due to the presence of polarons.[14] The absorption coefficients of **P1** and **P2** at 808 nm were 39.8 and 26.6 $Lg^{-1}cm^{-1}$, respectively, based on mass concentration. Both CPEs emit almost no fluorescence upon excitation and neither generated ROS under irradiation, as determined by using 9,10-anthracenediylbis(methylene)dimalonic acid (ABDA) as the indicator (see Fig. S1 the Supporting Information (SI)), indicating that non-radiative decay is the main pathway for excited state deactivation. Therefore, both CPEs predominantly convert absorbed light into heat.

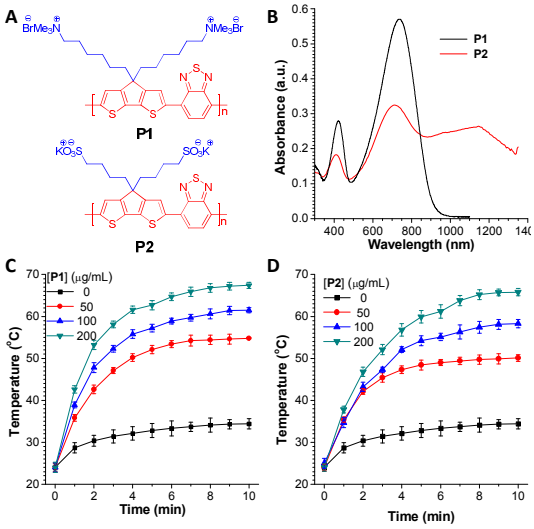

Fig. 1. A) Chemical structures and B) absorption spectra of **P1** and **P2** (10 μg/mL) in aqueous solution. Temperature changes of C) **P1** or D) **P2** aqueous solution under 808 nm laser irradiation (0.75 Wcm^{-2}).

Photothermal effects of **P1** and **P2** were investigated by examination of the temperature elevation upon laser excitation at 808 nm (0.75 Wcm^{-2}) with continuous wave diode laser (Figs. 1C and D). As control, the temperature of pure water under the same conditions was also tested, and revealed only a ~10 °C temperature increase starting at 24 °C after 10 min irradiation. Under the same level of irradiation, both **P1** and **P2** aqueous solutions showed higher and faster temperature increases. Indeed, one finds an increase of over 30 °C for 50 μg/mL of **P1** or **P2** upon 808 laser irradiation for 10 min. This temperature elevation increases with the increased concentrations of **P1** or **P2** in water. The flattening of the temperature increase with irradiation time and the nonlinear increase of temperature versus **P1** or **P2** concentration are largely due to high heat transfer to surroundings at high temperatures. Photothermal conversion efficiencies referring to the efficiency of transducing incident resonant energy to thermal energy was used to determine the ability of CPEs to transfer absorbed light to heat.[15] The photothermal conversion efficiency for **P1** and **P2** were determined to be 33 % and 32 %, respectively, according to the method developed by Roper et al (Fig. S2, see detailed calculations provided in the SI).[15a] These values are larger than those reported for the most widely used photothermal reagents, such as Au nanoshells (13%), Au nanorods (21%) or $Cu_{2-x}Se$ crystal (22%).[15] This temperature evolution experiment demonstrates that the narrow band gap CPEs can efficiently absorb 808 nm laser energy and produce thermal energy, features that make them promising agents for photothermal therapy.

The binding affinity of **P1** or **P2** towards bacteria and mammalian cells was examined. Gram-negative *E. coli* (ATCC 25922) was incubated with **P1** or **P2** at different concentrations

Journal of Materials Chemistry B Accepted Manuscript

This journal is © The Royal Society of Chemistry 20xx

Please do not adjust margins

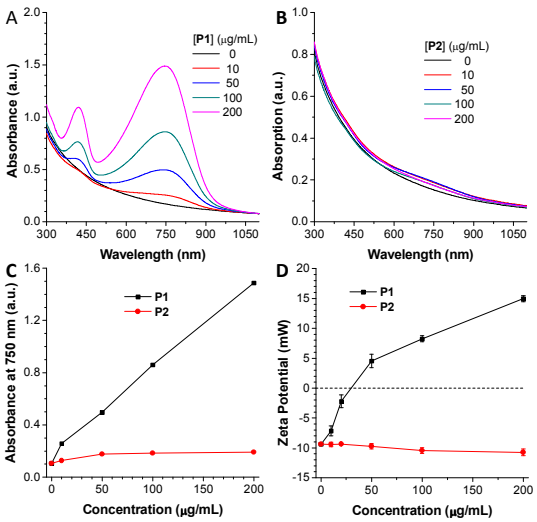

Fig. 2. Absorption spectra of the mixtures containing *E. coli* upon treatment with A) **P1** or B) **P2** at different concentrations. C) Plot of the absorbance at 750 nm versus **P1** or **P2** concentrations. D) Zeta potential changes of **P1** or **P2** treated *E. coli* at varied concentrations. The absorption and zeta-potential were measured after remove of free CPEs.

for 15 min at room temperature. Unbound CPEs were removed by centrifugation and washing of bacteria with 1× PBS buffer. Figs. 2A and B show the absorption spectra of the resulting *E. coli* suspensions after treatment with **P1** or **P2**. Their peak absorbance changes were plotted versus CPE concentrations (Fig. 2C). It is found that cationic **P1** shows high affinity to *E. coli*. Increasing the incubation concentration consequently increases the amount of **P1** binding to *E. coli*. In contrast, much less **P2** can be attached to *E. coli*, even at a concentration of 200 μg/mL (Fig. 2C). These studies reveal that hydrophobic interactions between *E coli* and the CPEs play only a minor role in binding to bacteria. Zeta-potential (ξ) changes of **P1** or **P2** treated *E. coli* were subsequently determined to study whether these CPEs were located at or inserted into the bacteria cell walls (Fig. 2D).[16] The *E. coli* surface is initially negatively charged with a ξ of ~-9.4 mV. Upon incubation with increased concentrations of **P1**, the ξ of *E. coli* is gradually changes from negative to positive ~15.1 mV, consistent with **P1** attaching to the surface of *E. coli*. On the other hand, **P2** treatment only leads to slightly decreased ξ, which reveals a weak interaction between **P2** and *E. coli*.

Similar binding experiments were applied to different bacteria, including Gram-positive *B. subtilis* (ATCC 33677), and drug-resistant bacteria Enterococcus faecium (Van A, genotype, ATCC 51559) and Enterococcus faecalis (Van B, ATCC 51299). Similar optical absorption and ξ changes were observed for Van A and Van B (Figs. S3 and S4 in the SI), indicating the generic adsorption of cationic **P1** onto the surface of different types of

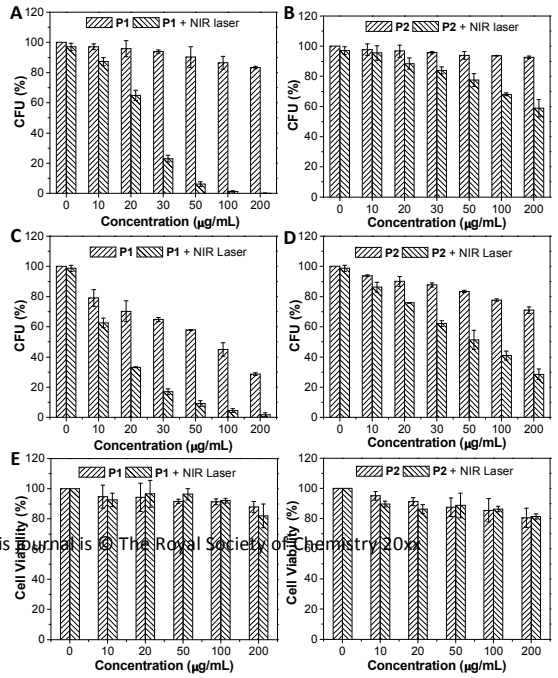

Fig. 3. Survival percentages of *E. coli* (A and B) or *B. subtilis* (C and D) after treatment with **P1** (A and C) or **P2** (B and D), and the viability of HeLa cells after treatment with **P1** (E) or **P2** (F) with or without 808 nm laser irradiation (6 min, 0.75 Wcm^{-2}).

bacteria. As for *B. subtilis*, although almost the same amounts of **P1** is bound as observed by the absorbance changes, the ξ increase of *B. subtilis* (from ~-12.0 to ~9.7 mV) is slower than that of *E coli* (from ~-9.4 to ~15.1 mV at **P1** concentration of 200 μg/mL) (Figs. 2D and S5). It is worth noting that *E. coli* generally contains an outer membrane that presents negatively charged lipopolysaccharide (LPS) outside the cell wall, while Gram-positive *B. subtilis* does not have the extra LPS layer.[11e,17] The thick and porous peptidoglycan cell walls of *B. subtilis* appears to aid **P1** insertion into the porous cell wall, maintaining the negatively charged surface, ultimately leading to a less pronounced ξ increase. In the absence of the LPS layer, bacteria-CPE hydrophobic interaction seems to play much more important roles in *B. subtilis* recognition, where anionic **P2** shows higher binding to *B. subtilis* relative to *E. coli* (Fig. S5). Finally, we note that **P1** or **P2** treated mammalian HeLa cancer cells show much less NIR absorbance and zeta potential changes (Fig. S6), suggesting a binding preference of **P1** towards bacteria over mammalian cells. Such a situation is consistent with previously established low binding affinity of QA to mammalian cells.[10e, 10f]

Motivated by the high affinity for bacterial cells and the excellent photothermal conversion of **P1**, we studied the antibacterial efficiency under NIR irradiation. The bacteria survival percentages were evaluated by the traditional agar plate colony-forming-unit (CFU) counting method (Fig. 3). Fig. 3A shows the results when *E. coli* is treated with **P1** in the dark. One finds minimal toxicity. The procedure only kills ~20% of the bacteria at a concentration of 200 μg/mL. Upon 808 nm laser irradiation, the *E. coli* survival percentage decreases rapidly to 66 and 0% upon increasing the **P1** concentration from 20 to 200 μg/mL, respectively (Figs. 3A and S7). **P1** shows much higher dark toxicity to *B. subtilis* as compared to *E coli*, where over 70% of *B. subtilis* is killed upon incubation with 200 μg/mL of **P1** (Fig. 3C). This dark toxicity difference should be ascribed to the extra LPS layer presented outside of the *E. coli* cell wall,[17b, 17c] which makes it less sensitive to QA compounds. Over 99% of *B. subtilis* can be killed when **P1** (100 μg/mL) is used together with 808 nm laser

Journal of Materials Chemistry B Accepted Manuscript

This journal is © The Royal Society of Chemistry 20xx

irradiation (Fig. S8). Similar results are also observed for drug resistance Van A and Van B (Figs. S9 and S10). As compared to **P1**, **P2** exhibits much lower bactericidal effects towards all the tested bacteria (Figs. 3B and D). At a concentration of 200 μg/mL, **P2** treatment under irradiation only shows killing efficiencies of ~40% and ~70% towards *E. coli* and *B. subtilis*, respectively (Figs. S11 and S12). Since both CPEs contain the same backbone and photothermal conversion efficiencies, the lower antibacterial effects of **P2** as compared to **P1** is attributed to the binding affinity differences between QA or sulfonate groups toward the bacteria. It should be noted that **P1** and **P2** showed much lower toxicity to mammalian cells under the same conditions (Figs. 3 E and 3F), making **P1** a step forward toward designing materials that selectively kill pathogen bacteria without affecting the normal functions of mammalian cells.

Insights into morphological changes of bacteria before and after treatment with **P1** and laser exposure were sought using field emission scanning electron microscopy. Sharp edges and smooth surfaces are observed for E. coli and B. subtilis control groups that were not subjected to any treatment (Figures 4A, D). Incubation with P1 in dark leads to rough membrane of E. coli, and new layers formed by P1 can even be observed on some E. coli (Figure 4B). When further exposed to 808 nm laser irradiation, the generated heat could cause protein denaturation and bubble formation,[18] leading to E. coli membrane damage, and the degree of membrane damage is gradually enhanced with increased P1 concentration and is accompanied with the observation of bacteria fragmentation and disintegration (Figure 4C). As for B. subtilis, P1 binding in dark distorts and wrinkles the cell membranes, and even produce holes on them (Figure 4E). Further damage is found after laser irradiation, which includes bubble formation and membrane swelling (Figure 4F). These SEM images provide direct information about the contact and photothermal damage

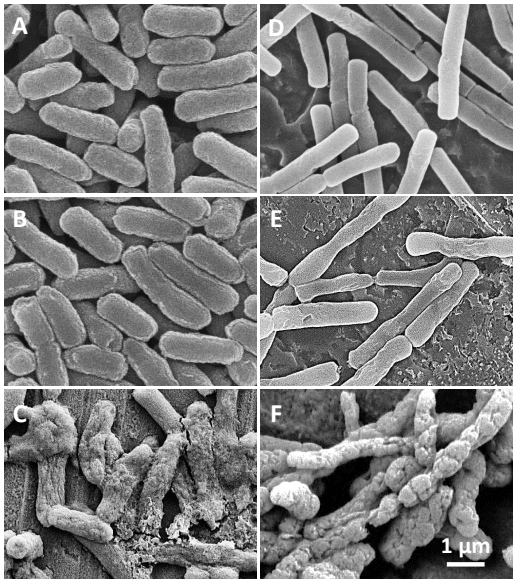

Fig. 4. Morphology of **P1** treated *E. coli* (A–C) and *B. subtilis* (D–F). (A, D) without **P1** under dark; (B, E) with **P1** (50 μg/mL) under dark; (C, F) with **P1** (50 μg/mL) and 808 nm laser irradiation (0.75 W cm^{-2}, 6 min). All figures share the same scale bar.

of antimicrobial CPEs to bacteria, which are consistent with the bacteria recognition and antibacterial experiments described in the preceding sections.

Conclusions

In summary, two CPEs that share the identical conjugated backbone structure have been studied within the context of photothermal killing of bacteria. **P1** with side chains bearing cationic QA groups showed high binding affinity towards all tested bacteria. In contrast, **P2** with anionic sulfonate groups exhibits low binding affinity to bacteria. The high affinity towards bacteria is mainly contributed by electrostatic binding to the cell wall by QA groups, and hydrophobic interactions play only a minor role. These features, together with excellent light-to-heat conversion ability under NIR laser irradiation makes **P1** an excellent bactericidal reagent, as confirmed by antibacterial experiments and SEM observation of cell damage. As sublethal use may lead to some defensive mechanisms of bacteria to resist QA-based AMPs,[19] it is thus of high importance to reduce the AMP concentration without compromising antimicrobial effects. Our antimicrobial CPEs inherently bring photothermal effects and traditional AMP functions into one molecule, which fulfill the requirement and should find their utility in antimicrobial applications. To the best of our knowledge, this is the first report of NIR absorbing water-soluble CPEs for photothermal killing of bacteria. This function also indicates that if photothermal CPEs can be further functionalized with antibodies, aptamers, or related recognition elements to identify specific tumor cells or bio-species for anticancer and other theranostic applications, they will offer new opportunities for further development of antimicrobial and anticancer materials.

Experimental Section

Materials

P1 was synthesized by treating its neutral precursor with bromohexyl side chains with excess trimethylamine, while **P2** was synthesized via Suzuki polymerization of anionic monomer directly. Dulbecco's Modified Eagle Medium (DMEM), 3-(4,5-dimethylthiazol-2-yl)-2,5-diphenyl tetrazolium bromide (MTT), trimethylamine, penicillin-streptomycin solution, fetal bovine serum (FBS) and trypsin-EDTA solution were purchased from Sigma-Aldrich. Milli-Q water was supplied by Milli-Q Plus System (Millipore Corporation, Bedford, USA). Phosphate-buffer saline (PBS; 10 ×) buffer with pH 7.4 (ultrapure grade) is a commercial product of 1st BASE Singapore. *E. coli* (ATCC 25922), *B. subtilis* (ATCC 33677), Enterococcus faecium (Van A, genotype, ATCC 51559), Enterococcus faecalis (Van B, ATCC

Journal of Materials Chemistry B Accepted Manuscript

This journal is © The Royal Society of Chemistry 20xx

Please do not adjust margins

51299), and HeLa cells were provided by American Type Culture Collection.

Characterization

UV-vis spectra were recorded on a Shimadzu UV-1700 spectrometer. Photoluminescence (PL) spectra were measured on a Perkin Elmer LS-55 equipped with a xenon lamp excitation source and a Hamamatsu (Japan) 928 PMT, using 90 degree angle detection for solution samples. All UV-vis and PL spectra were collected at 24 ± 1 °C. The morphology of bacteria was observed by scanning electron microscope (SEM) (JSM-6700F, JEOL, Japan) at an accelerating voltage of 5 kV. Bacteria were fixed on a stub with a double-sided sticky tape and then coated with a platinum layer using an autofine coater (JEOL, Tokyo, Japan) for 60 s in a vacuum at a current intensity of 30 mA. The surface zeta potential is measured by Zetasizer (Malvern Instruments, UK). Continuous wave diode laser (Diode Pumped Solid State Laser, Photonitech Pte Ltd) was used for photothermal experiment.

Bacteria Culture

A single colony of bacteria (*E coli*, *B. subtilis*, Van A or Van B) on a solid Luria Broth (LB) agar plate was transferred to 5 mL of LB liquid culture medium and culture at 37 °C overnight. The bacteria was then harvested by centrifuging at 5000 rpm for 5 min and washed with 1× PBS for three times. The bacteria pellet was then re-suspended in 1× PBS and the diluted to the desired density based on OD_{600} = 1.0.

Titration with *E coli*

The absorption spectra of **P1** and **P2** (10 μg/mL) were measured by UV-vis spectrometer (UV-1700, Shimadzu, Japan) in 1× PBS solution. *E coli* (OD_{600} = 0.1) was then added into **P1** or **P2** solution, and followed by measuring the absorbance. The absorption spectra of **P1** or **P2** in the presence of *E coli* were obtained by subtracting the spectra of *E coli* itself from the spectra of P1/P2 + *E coli.*

Bacteria Labelling

The bacteria suspended in 1× PBS buffer were incubated with **P1**/**P2** at varied concentrations. After 15 min incubation in dark, the unbound CPEs were removed by centrifugation and washing with 1× PBS for three times. The absorption spectra and zeta-potential changes of the bacteria were measured by UV-1700 and Zetasizer, respectively.

Antibacterial Assay

The antibacterial activity of **P1** and **P2** was accessed by the colony-forming unit (CFU) counting method. The cultured bacteria were harvested and re-suspended in 1× PBS solution (OD600 = 0.5). Then 90 μL of bacteria suspension was added into the centrifuge tube. **P1** and **P2** were then added into each tube to achieve the final concentration of 0, 10, 20, 30, 50, 100, 200 μg/mL. The total volume was kept at 100 μL, and the bacteria were incubated under dark at 37 °C for 15 min. The unbound CPEs were removed by centrifugation, and the bacteria were re-suspended in 1 × PBS. For the photothermal antimicrobial assay, the samples were irradiated to 808 nm laser (0.75 Wcm^{-2}) for 6 min. After laser irradiation, the bacterial suspensions were serially diluted 0.5 to 1×10^5 fold with 1 × PBS. 100 μL portion of the diluted bacterial suspension was spread on the solid LB agar plate and incubated at 37 °C for 16 h. The colonies formed were counted and the bacterial survival rates were determined by the ratio of colony forming unit (CFU) on the solid LB agar plate to that of the control under dark without CPE treatment.

Cell Culture

HeLa cancer cells were provided by American Type Culture Collection (ATCC). Cells were cultured in DMEM (Invitrogen, Carlsbad, CA) containing 10% FBS, and 1% penicillin-streptomycin. The cells were cultured in a humidified incubator with 5% CO_2 at 37 °C. Before experiment, the cells were cultured until confluence was reached.

Cell Labelling

HeLa cells were seeded in 6-well plate, and cultured to 80% confluence. **P1**/**P2** suspension in DMEM was added into the well. After 2 h incubation, HeLa cells were washed three times with PBS, and then harvested by trypsin, and re-suspended in 1× PBS. The absorbance and zeta potential changes are subsequently measured.

Cell Viability Measurement

HeLa cells were seeded in 96-well plates at a density of 40000 cells/mL. After overnight culturing, the media were replaced with **P1**/**P2** suspension in DMEM at different concentrations and incubated for 2 h in dark at 37 °C. The cells were then washed with fresh medium and 10% FBS was added. The cells were exposed to 808 nm laser (0.75 Wcm^{-2}) for 6 min. After irradiation, the cells were cultured overnight. In the parallel experiment, the cells were incubated with **P1** or **P2** in dark for 24 h. After overnight incubation, the cells were washed with 1× PBS, and 100 μL of freshly prepared MTT solution (0.5 mg/mL) was added into each well. After 3 h incubation, the MTT medium was removed, and filtered DMSO (100 μL) was added into each well. The absorbance at 570 nm was measured using a microplate reader (Genios Tecan). The untreated cells served as control and their viability is set as 100%.

SEM Measurement

Based on the antimicrobial experiments, the concentration of **P1** was determined to be 50 μg/mL for SEM measurement. Followed by irradiation, bacteria were centrifuged at 5000 rpm for 5 min to remove 1×PBS. The bacteria were then suspended in and fixed by 2.5% glutaraldehyde for 2-3 h at room temperature. The glutaraldehyde was removed by centrifuge, and the bacteria pellets were re-suspended in sterile water, and then 10 μL of bacteria suspension was spotted on to the SEM conducting paste. After natural drying in the air, the bacteria were dehydrated with a series of graded ethanol solution (30%, 50%, 70%, 80%, 90%, and 100% for 6 min). After

Journal of Materials Chemistry B Accepted Manuscript

drying overnight, the specimens were coated with platinum before SEM measurement.

Acknowledgements

The authors are grateful to the Singapore National Research Foundation (R279-000-444-281), SMART (R279-000-378-592), the Economic Development Board (Singapore-Peking-Oxford Research Enterprise, COY-15-EWI-RCFSA/N197-1), Institute of Materials Research and Engineering of Singapore (IMRE/12-8P1103) and US Air Force Office of Scientific Research (MURI FA9550-12-1-0002) for financial support.

References

1 (a) R. Khan, B. Islam, M. Akram, S. Shakil, A. A. Ahmad, S. M. Ali, M. Siddiqui, A. Khan, *Molecules* **2009,** *14*, 586-597; (b) B. S. Reisner, G. L. Woods, *J. Clin. Microbiol.* **1999,** *37*, 2024-2026; (c) H. Nikaido, *Ann. Rev. Biochem.* **2009,** *78*, 119-146; (d) M. Hartmann, P. Betz, Y. Sun, S. N. Gorb, T. K. Lindhorst, A. Krueger, *Chem. – Eur. J.* **2012,** *18*, 6485-6492; (e) H. K. Allen, J. Donato, H. H. Wang, K. A. Cloud-Hansen, J. Davies, J. Handelsman, *Nat. Rev. Microbiol.* **2010,** *8*, 251-259; (f) D. I. Andersson, D. Hughes, *Nat. Rev. Microbiol.* **2010,** *8*, 260-271; (g) K. E. Jones, N. G. Patel, M. A. Levy, A. Storeygard, D. Balk, J. L. Gittleman, P. Daszak, *Nature* **2008,** *451*, 990-993.

2(a) K. Kuroda, W. F. DeGrado, *J. Am. Chem. Soc.* **2005,** *127*, 4128-4129; (b) A. Muñoz-Bonilla, M. Fernández-García, *Prog. Polym. Sci.* **2012,** *37*, 281-339; (c) L. Timofeeva, N. Kleshcheva, *Appl. Microbiol. Biotechnol.* **2011,** *89*, 475-492; (d) T. Tashiro, *Macromol. Mater. Eng.* **2001,** *286*, 63-87.

3(a) R. F. Epand, B. P. Mowery, S. E. Lee, S. S. Stahl, R. I. Lehrer, S. H. Gellman, R. M. Epand, *J. Mol. Biol.* **2008,** *379*, 38-50; (b) H. Murata, R. R. Koepsel, K. Matyjaszewski, A. J. Russell, *Biomaterials* **2007,** *28*, 4870-4879; (c) M. Werthén, M. Davoudi, A. Sonesson, D. P. Nitsche, M. Mörgelin, K. Blom, K.; A. Schmidtchen, *J. Antimicrob. Chemother.* **2004,** *54*, 772-779; (d) C. Z.Chen, N. C. Beck-Tan, P. Dhurjati, T. K. van Dyk, R. A. LaRossa, S. L. Cooper, *Biomacromolecules* **2000,** *1*, 473-480; (e) E.-R. Kenawy, F. I. Abdel-Hay, A. E.-R. R. El-Shanshoury, M. H. El-Newehy, *Polym. Sci. Part A: Polym. Chem.* **2002,** *40*, 2384-2393; (f) B. Dizman, M. O. Elasri, L. J. Mathias, *J. Appl. Polym. Sci.* **2004,** *94*, 635-642.

4(a) Y. Zhang, H. Peng, W. Huang, Y. Zhou, D. Yan, *J. Colloid Interface Sci.* **2008,** *325*, 371-376; (b) H. Kong, J. Jang, *Langmuir* **2008,** *24*, 2051-2056; (c) C. Xing, Q. Xu, H. Tang, L. Liu, S. Wang, *J. Am. Chem. Soc.* **2009,** *131*, 13117-13124; (d) C. A. Strassert, M. Otter, R. Q. Albuquerque, A. Höne, Y. Vida, B. Maier, L. De Cola, *Angew. Chem. Int. Ed.* **2009,** *48*, 7928-7931; (e) B. Xing, T. Jiang, W. Bi, Y. Yang, L. Li, M. Ma,C.-K. Chang, B. Xu, E. K. L. Yeow, *Chem. Commun.* **2011,** *47*, 1601-1603; (f) S. A. Khan, A. K. Singh, D. Senapati, Z. Fan, P. C. Ray, *J. Mater. Chem.* **2011,** *21*, 17705-17709; (g) W.-C. Huang, P.-J. Tsai, Y.-C. Chen, *Small* **2009,** *5*, 51-56.

5(a) A. O. Patil, Y. Ikenoue, F. Wudl, A. J. Heeger, *J. Am. Chem. Soc.* **1987,** *109*, 1858-1859; (b) B. Liu, G. C. Bazan, *Conjugated Polyelectrolytes Fundamentals and Applications*. Wiley-VCH: Weinheim, 2013; (c) A. Duarte, K.-Y. Pu, B. Liu, B.; G. C. Bazan, *Chem. Mater.* **2010,** *23*, 501-515.

6(a) J. H. Seo, A. Gutacker, Y. Sun, H. Wu, F. Huang, Y. Cao, U. Scherf, A. J. Heeger, G. C. Bazan, *J. Am. Chem. Soc.* **2011,** *133*, 8416-8419; (b) C. Duan, K. Zhang, X. Guan, C. Zhong, H. Xie, F. Huang, J. Chen, J. Peng, Y. Cao, *Chem. Sci.* **2013,** *4*, 1298-1307; (c) J. Fang, B. H. Wallikewitz, F. Gao, G. Tu, C. Müller, G. Pace, R. H. Friend, W. T. S. Huck, *J. Am. Chem. Soc.* **2010,** *133*, 683-685.

7(a) K. Li, B. Liu, *Polym. Chem.* **2010,** *1*, 252-259; (b) Y. Wang, Y. Zhang, B. Liu, *Anal. Chem.* **2010,** *82*, 8604-8610; (c) Y. Wang, B. Liu, A. Mikhailovsky, G. C. Bazan, *Adv. Mater.* **2010,** *22*, 656-659; (d) B. Liu, G. C. Bazan, *Chem. Mater.* **2004,** *16*, 4467-4476; (e) K.-Y. Pu, B. Liu, *Adv. Funct. Mater.* **2009,** *19*, 277-284.

8(a) G. Feng, D. Ding, B. Liu, *Nanoscale* **2012,** *4*, 6150-6165; (b) K.-Y. Pu, B. Liu, *Adv. Funct. Mater.* **2011,** *21*, 3408-3423; (c) K.-Y. Pu, K. Li, B. Liu, *Chem. Mater.* **2010,** *22*, 6736-6741.

9Z. Zhou, T. S. Corbitt, A. Parthasarathy, Y. Tang, L. K. Ista, K. S. Schanze, D. G. Whitten, *J. Phys. Chem. Lett.* **2010**, 1, 3207-3212.

10(a) L. Lu, F. H. Rininsland, S. K. Wittenburg, K. E. Achyuthan, D. W. McBranch, D. G. Whitten, *Langmuir* **2005,** *21*, 10154-10159; (b) S. Chemburu, T. S. Corbitt, L. K. Ista, E. Ji, J. Fulghum, G. P. Lopez, K. Ogawa, K. S. Schanze, D. G. Whitten, *Langmuir* **2008,** *24*, 11053-11062; (c) L. Ding, E. Y. Chi, K. S. Schanze, G. P. Lopez, D. G. Whitten, *Langmuir* **2009,** *26*, 5544-5550; (d) H. Yuan, Z. Liu, L. Liu, F. Lv, Y. Wang, S. Wang, *Adv. Mater.* **2014,** *26*, 4333-4338; (e) C. Zhu, Q. Yang, L. Liu, F. Lv, S. Li, G. Yang, S. Wang, *Adv. Mater.* **2011,** *23*, 4805-4810; (f) C. Zhu, Q. Yang, L. Liu, S. Wang, *J. Mater. Chem.* **2011,** *21*, 7905-7912.

11(a) V. P. Zharov, K. E. Mercer, E. N. Galitovskaya, M. S. Smeltzer, *Biophys. J. 90*, 619-627; (b) K. A. Sukalski, T. P. LaBerge, W. T. Johnson, *Free Radical Biol. Med.* **1997,** *22*, 835-842; (c) J. H. Calhoun, J. A. Cobos, J. T. Mader, *Orthoped. Clin. NA* **1991,** *22*, 467-471.

12 (a) C. Loo, A. Lowery, N. Halas, J. West, R. Drezek, *Nano Lett.* 2005, **5**, 709-711; (b) X. Huang, I. H. El-Sayed, W. Qian, M. A. El-Sayed, *J. Am. Chem. Soc.* 2006, **128**, 2115-2120; (c) J.-W. Kim, E. I. Galanzha, E. V. Shashkov, H.-M. Moon, V. P. Zharov, *Nat. Nanotechnol.* 2009, **4**, 688-694; (d) K. Yang, S. Zhang, G. Zhang, X. Sun, S.-T. Lee, Z. Liu, *Nano Lett.* 2010, **10**, 3318-3323.

13(a) F. Van Bambeke, R. Reinert, P. Appelbaum, P. Tulkens, W. Peetermans, *Drugs* **2007,** *67*, 2355-2382; (b) A. B. Mochon, O. B. Garner, J. A. Hindler, P. Krogstad, K. W. Ward, M. A. Lewinski, J. K. Rasheed, K. F. Anderson, B. M. Limbago, R. M. Humphries, *J. Clin. Microbiol.* **2011,** *49*, 1667-1670; (c) J. L. Martinez, F. Baquero, D. I. Andersson, *Nat. Rev. Microbiol.* **2007,** *5*, 958-965; (d) G. D.Wright, *Chem. Commun.* **2011,** *47*, 4055-4061.

14(a) Z. B. Henson, Y. Zhang, T.-Q. Nguyen, J. H. Seo, G. C. Bazan, *J. Am. Chem. Soc.* **2013,** *135*, 4163-4166; (b) C.-K. Mai, H. Zhou, Y. Zhang, Z. B. Henson, T.-Q. Nguyen, A. J. Heeger, G. C. Bazan, *Angew. Chem. Int. Ed.* **2013,** *125*, 13112-13116; (c) C.-K. Mai, R. A. Schlitz, G. M. Su, D. Spitzer, X. Wang, S. L. Fronk, D. G. Cahill, M. L. Chabinyc, G. C. Bazan, *J. Am. Chem. Soc.* **2014,** *136*, 13478-13481.

15(a) D. K. Roper, W. Ahn, M. Hoepfner, *J. Phys. Chem. C* **2007,** *111*, 3636-3641; (b) Q. Tian, F. Jiang, R. Zou, Q. Liu, Z. Chen, M. Zhu, S. Yang, J. Wang, J. Wang, J. Hu, *ACS Nano* **2011,** *5*, 9761-9771; (c) C. M. Hessel, V. P. Pattani, M. Rasch, M. G. Panthani, B. Koo, J. W. Tunnell, B. A. Korgel, *Nano Lett.* **2011,** *11*, 2560-2566.

16(a) M. C.van Loosdrecht, J. Lyklema, W. Norde, G. Schraa, A. J. Zehnder, *Appl. Environ. Microbiol.* **1987,** *53*, 1898-1901; (b) W. W. Wilson, M. M. Wade, S. C. Holman, F. R. Champlin, *J. Microbiol. Methods* **2001,** *43*, 153-164; (c) P. Gilbert, D. J. Evans, E. Evans, I. G. Duguid, M. R. W. Brown, *J. Appl. Bacteriol.* **1991,** *71*, 72-77.

17(a) S. Chambon, A. Rivaton, J.-L. Gardette, M. Firon, *J. Polym. Sci. Part A: Polym. Chem.* **2009,** *47*, 6044-6052; (b) S. R. Coats, T.-T. T. Pham, B.W. Bainbridge, R. A. Reife, R. P. Darveau, *J. Immunol.* **2005,** *175*, 4490-4498; (c) L. M.

Journal of Materials Chemistry B Accepted Manuscript

This journal is © The Royal Society of Chemistry 20xx

Prescott, D. A. Klein, J. P. Harley, *Microbiology*. 5th ed.; The McGraw-Hill Companies: Columbus, 2002.

18(a) V. P. Zharov, K. E. Mercer, E. N. Galitovskaya, M. S. Smeltzer, *Biophys. J.* **2006,** *90*, 619-627; (b) P. C. Ray, S. A. Khan, A. K. Singh, D. Senapati, Z. Fan, *Chem. Soc. Rev.* **2012,** *41*, 3193-3209.

19(a) G. Sundheim, S. Langsrud, E. Heir, A. L. Holck, *Int. Biodeterior. Biodegrad.* **1998,** *41*, 235-239; (b) J.-Y. Maillard, *Ther. Clin. Risk Manage.* **2005,** *1*, 307-320; (c) B. Aase, G. Sundheim, S. Langsrud, L. M. Rørvik, *Int. J. Food Microbiol.* **2000,** *62*, 57-63.

20

Journal of Materials Chemistry B Accepted Manuscript